

KVALITA OVZDUŠÍ V OBYDLENÉ ZÓNĚ: VLIV TROJROZMĚRNÉHO PROSTORU MĚSTSKÉ ZÁSTAVBY

AIR QUALITY AT PEDESTRIAN ZONE: THE ROLE OF URBAN-ARRAY THREE-DIMENSIONALITY

Štěpán Nosek^{a*}, Radka Kellnerová^a, Hana Chaloupecká^{ab}, Michala Jakubcová^a, Zbyněk Jaňour^a

^a Institute of Thermomechanics of the CAS, v. v. i., Dolejškova 1402/5, Prague, Czech Republic

^b Charles University in Prague, Faculty of Mathematics and Physics, Department of Atmospheric Physics, V Holešovičkách 2, Prague, Czech Republic

*Corresponding author; e-mail: nosek@it.cas.cz, tel.: +420 266 053 382

Abstract

Air quality at pedestrian level of two different urban arrays for two wind directions was studied experimentally in a wind-tunnel. Both urban arrays were designed according to typical European cities, formed by courtyard-type buildings with pitched roofs. While the first urban array had constant roof height, the second had variable roof height along all walls. The pollution was simulated by means of ground-level line source in the middle of the urban arrays. The concentrations were measured by a flame ionization detector at horizontal planes at the pedestrian level within the streets and courtyards at the vicinity of the line source. Results of the time and spatial averaged concentration reveal that both wind direction and three-dimensionality of the urban morphology are important parameters influencing the air quality at the pedestrian zones within the urban areas.

Key words: *air quality, pedestrian level, court-yard buildings, wind-tunnel*

1 INTRODUCTION

Understanding of pollutant dispersion within urban areas is of importance due to many health-related issues. As the majority of the population lives in cities, this importance is more crucial. Urban areas consisting of buildings which form streets and intersections act as aerodynamic roughness which in turn might have unfavourable, but also favourable effect, on pollutant dispersion. Depending on the wind direction above the roof level, several flow patterns develop within the street canyons and intersections as has been observed and established by numerous field (e.g., Louka et al. 2000; Dobre et al. 2005; Balogun et al. 2010; Klein & Galvez 2014), reduced-scale wind-tunnel (e.g., Pavageau & Schatzmann 1999; Klein et al. 2007; Carpentieri et al. 2009; Kellnerová et al. 2012; Addepalli & Pardyjak 2014), and numerical (e.g., Leitl & Meroney 1997; Xie et al. 2005; Coceal et al. 2006; Tominaga & Stathopoulos 2013; Michioka et al. 2014; Liu et al. 2015) studies.

When the above-roof wind is perpendicular to the street, the main recirculation vortex with rotation axis parallel to the street mainly develops at the centre of the street canyon. This vortex might be attended with smaller vortices at both leeward and windward corners of the canyon and completely vanishes due to helical vortices with vertical axis at both lateral sides where the canyon is adjoining to the intersections. In case of above-roof winds parallel with the street canyon, the channelled flow dominates within the canyon and is the most favourable regarding the ventilation if the source of the pollution is not situated upstream.

However, in real cases the approaching wind rarely persists in perpendicular or parallel direction to the street axis. For these oblique winds more complex flow patterns such as combination of cross-canyon recirculation with channelled flow within the street canyons can be observed (Belcher, 2005). These street-canyon flow characteristics are getting more complex if the roof height is not uniform along the either sides of the canyon as was demonstrated by field (Longley et al. 2004; Balogun et al. 2010), wind-tunnel (Klein et al. 2007; Nosek et al. 2016) and numerical (Gu et al. 2011) studies. Moreover, the adjoining intersections play another crucial role in forming the flows in the canyons as suggested by several field studies (Robins et al. 2002; Klein et al. 2007; Barlow et al. 2009). However, due to ever-changing meteorological conditions the field studies lack the systematic manner and the effects of urban geometry on pollutant dispersion are still poorly understood.

In order to better understand the later mentioned issue, we present in this paper the wind-tunnel investigation of combined effects of urban geometry and flow conditions. Namely two different urban morphologies and approach wind directions, on pollutant dispersion at pedestrian level of the street-canyons, the adjoining intersections, and the court-yards.

2 METHODOLOGY

2.1. Experimental set-up

For detailed description of the basic part of the experimental set-up, we refer the reader to our previous work (Nosek et al. 2016). Briefly, we used the open low-speed wind tunnel (cross-sectional dimensions: 1.5 x 1.5m) of the Institute of Thermomechanics of the Czech Academy of Sciences in Nový Knín. Because the pollutant dispersion in urban areas is related to the atmospheric boundary layer developed above such type of terrain roughness, we simulated the appropriate approaching boundary layer before the model of urban area at 20.5 long development section of the wind-tunnel. This involved not only the fulfilment of an aerodynamic parameters of the simulated boundary layer (roughness length, displacement height, friction velocity) according to recommended standards (e.g, VDI 2000), but also the corresponding characteristics of turbulence, such as spectrum and length scales (not shown here), which are crucial for the atmospheric dispersion.

Overall, the experiment was conducted under neutrally-stratified conditions at sufficiently height Reynolds number, $Re = 24400$ (based on the free-stream reference velocity, U_{ref} , and average height of the modelled urban array, H_m), in order to fulfil the independence of flow regime on Re . For both urban arrays this leads to the urban models of a scale of 1:400, each formed by evenly spaced 8 x 4 courtyard-type buildings of constant length, L , and width, W (*Fig. 1*).

The difference between the modelled urban arrays consisted in the height of the pitched roof of the court-yard buildings. While the reference urban model, A1, had the constant roof height ($H = H_m$, equal to dimensionless height $z/H = 1.0$), the second urban model, A2, had arbitrarily distributed the roof height along each building wall. The roof-height non-uniformity in the model A2 was distributed such that each of the building had four and two segments of different heights ($z/H = 0.8, 1$ or 1.2) along its longer (L) and shorter (W) wall, respectively (*Fig. 2*). Meanwhile, the average height, plan and frontal solidities of both urban arrays were the same.

We addressed the pollution from traffic and simulated it by a ground-level line source emitting homogeneously the passive gas ethane in the fourth span-wise avenue (parallel with y coordinate). The line source continuously runs across all stream-wise avenues (parallel with y

coordinate) in each of the urban models (Fig. 2), hence emitting the pollutant evenly not only at the street canyons but also at the intersections. For concentration measurement, we used a Fast-Response Flame Ionisation Detector (FFID), type Cambustion Ltd. HFR400. The FFID sampling frequency was set to 0.5 kHz corresponding to its tested response time 2 ms. According to the central moment independence tests, the sampling time for each measuring point was set to 60 s.

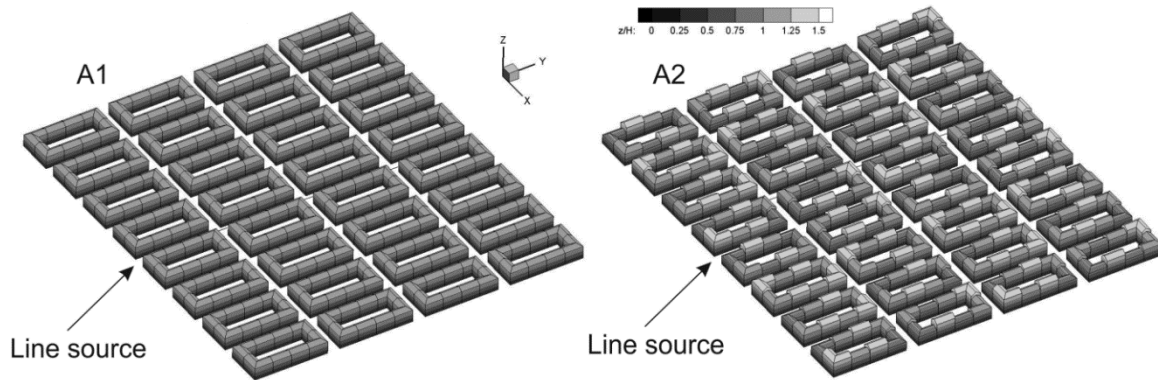


Figure 1 Schemes of studied urban models. Left: urban model (A1) of uniform height. Right: urban model (A2) of non-uniform height. The grey contour refers to the dimensionless height (z/H) of the building. The 3D coordinates in the middle refer to the wind-tunnel coordinate system.

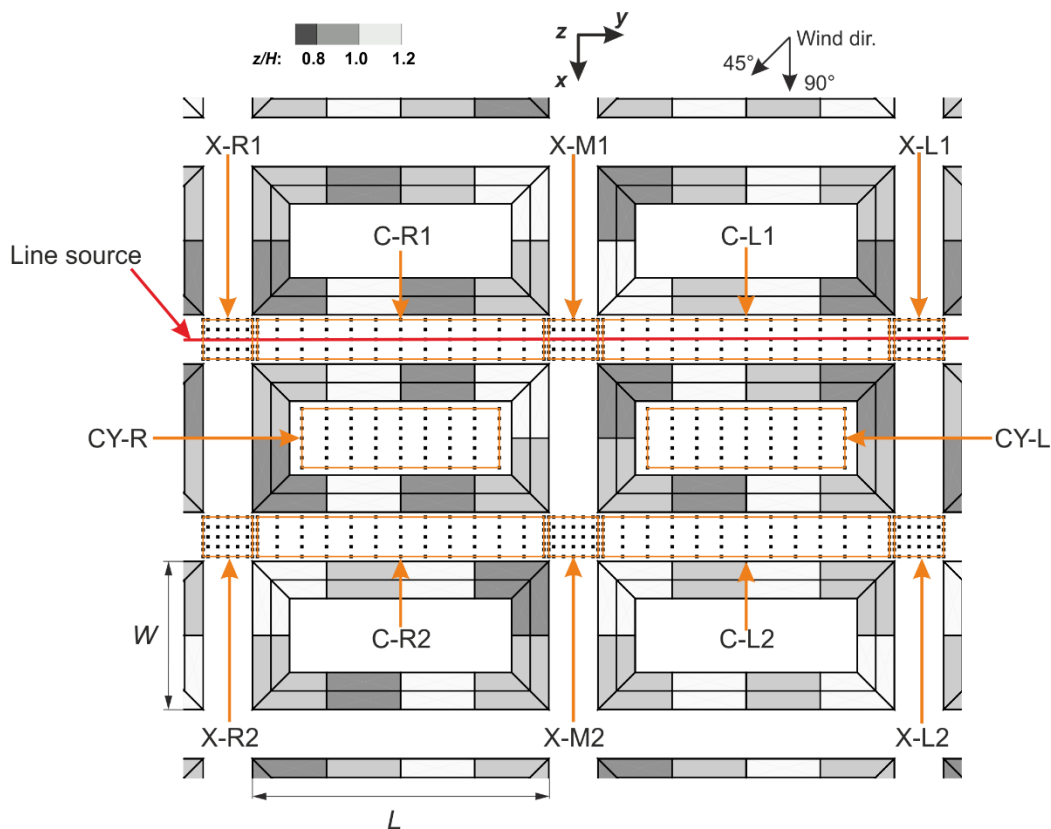


Figure 2 The scheme of measured points (black dots) at pedestrian level within the labelled areas (orange rectangles) of the urban array A2. The ground-level line source positioned in the middle of the fourth span-wise avenue is denoted by red line. The used right-hand Cartesian coordinate system and simulated both win directions are denoted at the top.

2.2 Data analysis

The measurement points for selected areas regarding the studied near-field pollutant dispersion at the pedestrian level ($z/H = 0.1$) of the non-uniform urban array A2 are depicted in *Fig. 2*. Due to the previously verified flow symmetry of the uniform urban array A1, we investigated only the areas C-R1, X-M1, C-R2, X-M2 and CY-R in the case of wind direction parallel with the stream-wise avenues (0° relative to the buildings). In the case of oblique wind direction (45° relative to the buildings), another two areas (the intersections) X-R1 and X-R2 were investigated in urban array A1 to observe the effect of potential advection of the pollutant downstream from the line source.

In order to compare the simulated cases quantitatively, we performed the spatial averaging of the concentration fields (not shown here) for each of the investigated area and each simulated case as

$$\langle C^* \rangle_i = \frac{1}{A_i} \iint_{A_i} C^* dydx, \quad (1)$$

where A_i is the i investigated area counting the simulated case, and C^* is the time-averaged concentration normalized according to the VDI guideline (VDI, 2000) as

$$C^* = \frac{CU_{ref}H_mL_s}{Q}, \quad (2)$$

where C is the measured mean concentration, U_{ref} is the reference velocity corresponding to the wind-tunnel free-stream velocity, H_m is the average height of the urban arrays, L_s is the length of the source and Q is the volume rate of ethane flow from the entire line source.

We also analysed the temporal variability of the dimensionless concentration at corresponding i area by means of temporal standard deviation as

$$\sigma_{Ti} = \sqrt{\langle c^{*'} c^{*'} \rangle}, \quad (3)$$

where $c^{*'}$ is the instantaneous fluctuation of the dimensionless concentration, overbar denotes the time average and the angled brackets denote the spatial average over an i area according to Eq. 1.

3 RESULTS

3.1. Spatially averaged concentration

In *Table 1* are presented the results of the spatially averaged concentration $\langle C^* \rangle$ for each investigated area and case. The last two columns represent the ratio between the reference case A1 and A2 ($\langle C^* \rangle_{A1} / \langle C^* \rangle_{A2}$). We calculated these ratios also for the areas of the urban array A1 where we did not measure because the similarity tests revealed that urban array is symmetrical for both flow and dispersion patterns (the mean percentage of difference between the symmetrically positioned measured points was around 2% and lower than the error of the concentration measurement, 4%). Thus, for ratio computations, we used the reference areas in the case of urban array A1 as: C-R1 for C-L1, C-R2 for C-L2, X-M1 for X-R1 and X-L1, X-M2 for X-R2 and X-L2, and CY-R for CY-L (see *Fig. 2*).

The biggest difference between the urban array of the constant roof height and that of the variable roof height can be observed in the case of perpendicular wind direction and for the street canyons where the line source is presented (first row and fifth column in *Table 1*).

Table 1 Spatially-averaged dimensionless concentrations, $\langle C^* \rangle$, for each measured area and wind direction. The bolted values denote appreciable high levels of $\langle C^* \rangle$, or appreciable high or low ratios of $\langle C^* \rangle$.

	A1-90	A1-45	A2-90	A2-45	A1-90/A2-90	A1-45/A2-45
C-R1	78.4	64.5	38.9	53.7	2.0	1.2
C-R2	5.0	6.0	2.9	5.0	1.7	1.2
C-L1	–	–	62.1	48.7	1.3	–
C-L2	–	–	5.2	4.3	1.0	–
X-M1	70.7	229.0	94.8	195.3	0.7	1.2
X-R1	–	221.1	96.9	197.2	0.7	1.1
X-L1	–	–	84.8	124.4	0.8	–
X-M2	34.1	18.4	38.3	18.3	0.9	1.0
X-R2	–	25.2	33.3	23.8	1.0	–
X-L2	–	–	39.9	26	0.9	–
CY-R	5.5	5.4	4.9	5.3	1.1	1.0
CY-L	–	–	5.7	3.0	1.0	–

Table 2 Temporal fluctuations of dimensionless concentration, σ_T , for each measured area and wind direction. σ_T is normalized by the $\langle C^* \rangle$. The bolted values denote appreciable high levels of σ_T , or appreciable high or low ratios of σ_T .

	A1-90	A1-45	A2-90	A2-45	A1-90/A2-90	A1-45/A2-45
C-R1	0.84	1.19	0.88	1.25	1.0	1.0
C-R2	0.76	0.57	0.70	0.04	1.1	13.6
C-L1	–	–	0.75	1.27	1.1	–
C-L2	–	–	0.67	0.07	1.1	–
X-M1	2.12	1.34	1.49	1.47	1.4	1.2
X-R1	–	1.31	1.64	1.33	1.3	1.1
X-L1	–	–	1.71	1.56	1.2	–
X-M2	1.27	0.83	0.93	1.00	1.4	1.0
X-R2	–	0.60	0.90	0.83	1.2	–
X-L2	–	–	0.96	1.18	1.3	–
CY-R	0.52	0.50	0.55	0.43	1.0	1.0
CY-L	–	–	0.58	0.57	0.9	–

The spatially averaged concentration $\langle C^* \rangle$ is two times higher in the canyon of constant roof height (A1-90-R1) than that of variable roof height (A2-90-R1). While the concentrations exponentially decrease in the first canyons downstream from the release location for both urban arrays, there is still difference between the spatially averaged concentrations (first row and fifth

column in *Table 1*) in spite of that compared values are small and of minor importance. If we look at street canyon A2-90-L1, the $\langle C^* \rangle$ is about 20% lower than that of reference canyon A1-90-R1 (third row and fifth column in *Table 1*). There is no other appreciable difference in spatially averaged concentration between the reference urban array and urban array with variable roof.

This and other results from *Table 1* clearly illustrate that: (1) urban array with variable roof height along all buildings' walls better ventilates the line source; (2) it is important to investigate each of the street canyon and intersection of an uneven urban array separately with respect to air quality at the pedestrian zone; (3) the highest $\langle C^* \rangle$ were observed at intersections for oblique wind direction and were appropriately two times higher than those for perpendicular wind direction, irrespective of studied urban array; (4) the lowest $\langle C^* \rangle$ were observed for courtyards, except of the courtyard CY-L of the urban array A2 where the $\langle C^* \rangle$ was slightly higher than that for the canyon C-L2 of the same urban array ; (5) for oblique wind direction the differences between both investigated urban arrays vanished due to higher mixed and complex flow.

3.2. Temporal variability of concentration

In *Table 2* are presented the temporal fluctuations of concentration, σ_T , normalized by $\langle C^* \rangle$, for each investigated area and case. Thus, the value in *Table 2* shows how many times the time-averaged concentration fluctuations deviate from the concentration mean. The last two columns represent again the ratio between the reference case A1 and A2 ($\sigma_{TA1} / \sigma_{TA2}$). Overall, there are no such appreciable differences in σ_T compared to previously investigated $\langle C^* \rangle$. However, results from *Table 2* clearly indicate that temporal variability of the concentration is generally lower for the case of urban array with variable roof height than that of constant roof height, irrespective of the wind direction. This points out on better mixed airflow, hence better ventilation and air quality of urban array of uneven roof height.

4 CONCLUSION

We demonstrated the effect of urban-array three-dimensionality on air quality at the pedestrian level on two wind directions and two urban arrays of the same regular layout, but of different roof-height morphology. The results of the near-field pollutant dispersion of the homogenous line source simulating the even traffic clearly show that regular array can be treated only as regular if the buildings are regularly spaced and have the same dimensions. For instance, if such regular array will change the roof height along its all buildings' walls, the better air quality is achieved, irrespective of the wind direction. Irrespective of studied urban array, the highest spatially averaged concentrations were observed at intersections and were two times higher for the case of oblique wind direction, suggesting higher complexity of the flow. Regarding both, the temporal variability of the concentration fluctuations and spatially averaged concentration, the best air-quality area was observed for the first street canyons downstream from the line source of the urban array with uneven roof height in the case of oblique wind direction. These results are relevant not only for urban planners but also for rescue planners in cases of accidental or deliberate release of harmful substances within similar urban array.

Acknowledgements

This contribution was supported by the Czech Science Foundation GACR (project GAP15-18964S) and the institutional support RVO: 61388998.

Sources

1. ADDEPALLI, B. & PARDYJAK, E. R.: A study of flow fields in step-down street canyons. *Environmental Fluid Mechanics*, 2014, pp. 439–481. ISSN: 1567-7419.
2. BALOGUN, A. A. et al.: In-Street Wind Direction Variability in the Vicinity of a Busy Intersection in Central London. *Boundary-Layer Meteorology*, 2010, 136(3), pp. 489–513. ISSN: 0006-8314.
3. BARLOW, J. F. et al.: Referencing of street-level flows measured during the DAPPLE 2004 campaign. *Atmospheric Environment*, 2009, 43(34), pp. 5536–5544. ISSN: 1352-2310.
4. BELCHER, S. E.: Mixing and transport in urban areas. *Philosophical transactions. Series A, Mathematical, physical, and engineering sciences*, 2005, 363(October), pp. 2947–2968.
5. CARPENTIERI, M., ROBINS, A. G. & BALDI, S.: Three-Dimensional Mapping of Air Flow at an Urban Canyon Intersection. *Boundary-Layer Meteorology*, 2009, 133(2), pp. 277–296. ISSN: 0006-8314.
6. COCEAL, O. et al.: Mean flow and turbulence statistics over groups of urban-like cubical obstacles. *Boundary-Layer Meteorology*, 2006, 121(3), pp. 491–519. ISSN: 0006-8314.
7. DOBRE, A. et al.: Flow field measurements in the proximity of an urban intersection in London, UK. *Atmospheric Environment*, 2005, 39(26), pp. 4647–4657. ISSN: 1352-2310.
8. GU, Z.-L. et al.: Effect of uneven building layout on air flow and pollutant dispersion in non-uniform street canyons. *Building and Environment*, 2011, 46(12), pp. 2657–2665. ISSN: 0360-1323.
9. KELLNEROVÁ, R. et al.: PIV measurement of turbulent flow within a street canyon: Detection of coherent motion. *Journal of Wind Engineering and Industrial Aerodynamics*, 2012, 104-106, pp. 302–313. ISSN: 0167-6105.
10. KLEIN, P., LEITL, B. & SCHATZMANN, M.: Driving physical mechanisms of flow and dispersion in urban canopies. *International Journal of Climatology*, 2007, 27 (September), pp. 1887–1907. ISSN: 1097-0088.
11. KLEIN, P. M. & GALVEZ, J. M.: Flow and turbulence characteristics in a suburban street canyon. *Environmental Fluid Mechanics*, 2014, 15(2), pp. 419-438. ISSN: 1567-7419.
12. LEITL, B. M. & MERONEY, R. N.: Car exhaust dispersion in a street canyon Numerical critique. *Journal of Wind Engineering and Industrial Aerodynamics*, 1997, 67, pp. 293–304. ISSN: 0167-6105.
13. LIU, C.-H., NG, C.-T. & WONG, C. C. C.: A theory of ventilation estimate over hypothetical urban areas. *Journal of Hazardous Materials*, 2015, 296, pp. 9–16. ISSN: 0304-3894.

14. LONGLEY, I. D. et al.: Short-term measurements of airflow and turbulence in two street canyons in Manchester. *Atmospheric Environment*, 2004, 38(1), pp. 69–79. ISSN: 1352-2310.
15. LOUKA, P., BELCHER, S. E. & HARRISON, R. G.: Coupling between air flow in streets and the well-developed boundary layer aloft. *Atmospheric Environment*, 2000, 34(16), pp. 2613–2621. ISSN: 1352-2310.
16. MICHIOKA, T., TAKIMOTO, H. & SATO, A.: Large-Eddy Simulation of Pollutant Removal from a Three-Dimensional Street Canyon. *Boundary-Layer Meteorology*, 2014, 150, pp. 259–275. ISSN: 0006-8314.
17. NOSEK, Š. et al.: Ventilation Processes in a Three-Dimensional Street Canyon. *Boundary-Layer Meteorology*, 2016, 159, pp. 259–284. ISSN: 0006-8314.
18. PAVAGEAU, M. & SCHATZMANN, M.: Wind tunnel measurements of concentration fluctuations in an urban street canyon. *Atmospheric Environment*, 1999, 33, pp. 3961–3971. ISSN: 1352-2310.
19. PERRET, L., BLACKMAN, K. & SAVORY, E.: Combining Wind-Tunnel and Field Measurements of Street-Canyon Flow via Stochastic Estimation. *Boundary-Layer Meteorology*, 2016, pp. 1–27. ISSN: 0006-8314.
20. ROBINS, A. et al.: Spatial variability and source-receptor relations at a street intersection. *Water, Air, & Soil Pollution: Focus*, 2002, 2(5), pp. 381–393. ISSN: 1567-7230.
21. TOMINAGA, Y. & STATHOPOULOS, T.: CFD simulation of near-field pollutant dispersion in the urban environment: A review of current modeling techniques. *Atmospheric Environment*, 2013, 79, pp. 716–730. ISSN: 1352-2310.
22. VDI Verein Deutcher Ingenieure ed.: *Physical modelling of flow and dispersion processes in the atmospheric boundary layer - application of wind tunnels*. 2000, VDI Verein Deutcher Ingenieure, Düsseldorf.
23. XIE, X., HUANG, Z. & WANG, J. S.: Impact of building configuration on air quality in street canyon. *Atmospheric Environment*, 2005, 39(25), pp. 4519–4530. ISSN: 1352-2310.